AD_____

Award Number: DAMD17-01-1-0689

TITLE: The BESCT Lung Cancer Program (Biology, Education, Screening, Chemoprevention, and Treatment)

PRINCIPAL INVESTIGATOR: Waun K. Hong, M.D.
Fadlo R. Khuri, M.D.

CONTRACTING ORGANIZATION: The University of Texas
M.D. Anderson Cancer Center
Houston, TX 77030

REPORT DATE: March 2009

TYPE OF REPORT: Final Addendum

PREPARED FOR: U.S. Army Medical Research and Materiel Command
Fort Detrick, Maryland 21702-5012

REPORT DOCUMENTATION PAGE

Form Approved
OMB No. 0704-0188

1. REPORT DATE	2. REPORT TYPE	3. DATES COVERED
01-03-2009	Final Addendum	15 Feb 2008– 14 Feb 2009

4. TITLE AND SUBTITLE

The BESCT Lung Cancer Program (Biology, Education, Screening, Chemoprevention, and Treatment)

5a. CONTRACT NUMBER

5b. GRANT NUMBER
DAMD17-01-1-0689

5c. PROGRAM ELEMENT NUMBER

6. AUTHOR(S)

Waun K. Hong, M.D.
Fadlo R. Khuri, M.D.

Email: whong@mdanderson.org

5d. PROJECT NUMBER

5e. TASK NUMBER

5f. WORK UNIT NUMBER

7. PERFORMING ORGANIZATION NAME(S) AND ADDRESS(ES)

The University of Texas
M.D. Anderson Cancer Center
Houston, TX 77030

8. PERFORMING ORGANIZATION REPORT NUMBER

9. SPONSORING / MONITORING AGENCY NAME(S) AND ADDRESS(ES)
U.S. Army Medical Research and Materiel Command
Fort Detrick, Maryland 21702-5012

10. SPONSOR/MONITOR'S ACRONYM(S)

11. SPONSOR/MONITOR'S REPORT NUMBER(S)

12. DISTRIBUTION / AVAILABILITY STATEMENT
Approved for Public Release; Distribution Unlimited

13. SUPPLEMENTARY NOTES

14. ABSTRACT

BESCT program aims to define molecular abnormalities contributing to lung cancer initiation and progression and to develop innovative therapeutic approaches for this cancer. Our specific aims are 1) to understand molecular alterations in lung cancer, 2) to develop chemoprevention strategies for lung cancer, and 3) to implement experimental molecular therapeutic approaches for lung cancer treatment.

15. SUBJECT TERMS
Lung Cancer, genetic alterations, chemoprevention, molecular therapy

16. SECURITY CLASSIFICATION OF:			17. LIMITATION OF ABSTRACT	18. NUMBER OF PAGES	19a. NAME OF RESPONSIBLE PERSON
a. REPORT	b. ABSTRACT	c. THIS PAGE			19b. TELEPHONE NUMBER *(include area code)*
U	U	U	UU	27	USAMRMC

Standard Form 298 (Rev. 8-98)
Prescribed by ANSI Std. Z39.18

TABLE OF CONTENTS

INTRODUCTION – BESCT Project Extension

The BESCT program developed in 2001 aimed to define molecular abnormalities contributing to lung cancer initiation and progression and to develop innovative therapeutic approaches for this cancer. The specific aims were as follows:

- To understand molecular alterations in lung cancer
- To develop chemoprevention strategies for lung cancer
- To implement experimental molecular therapeutic approaches for lung cancer treatment

Difficulties resulting from the purchase of Ligand Pharmaceuticals by Eisai led to the conclusion that the clinical trial planned and agreed upon previously would not be able to be completed. Thus, building upon the preclinical work in BESCT and in BATTLE, we proposed the revised aims to replace Specific Aim 2.1, which we believe will be synergistic with both studies and accomplish the original intent of the BESCT program.

We propose to build on our initial work showing that combining an mTOR inhibitor with PI3 kinase inhibitors led to accelerated cell growth inhibition. The development of PI3 kinase inhibitors in lung cancer has had an uncertain course; however, inhibition of IGFR by either a monoclonal antibody or tyrosine kinase inhibitors (TKIs) is undergoing accelerated development in the lung cancer arena. With a strong track record of developing agents both in prevention [1-3] and therapy [4-16], we propose mechanistic work in cell lines to understand the basis of the enhanced pharmacologic dependence on the Akt/mTOR axis in lung cancer cell lines treated with rapamycin or its analogs, such as RAD001. We will subsequently study the biology behind the accelerated cell growth inhibition kinetics when we introduce an IGFR inhibitor after initial treatment with rapamycin. Importantly, we will study the optimal treatment sequence for these agents to see whether the maximum effect is obtained when Akt is first paradoxically upregulated by rapamycin blockade, followed by treatment with IGFR inhibitors. We then plan to take this combination into a biomarker-driven phase I clinical trial incorporating serial biopsies of accessible tumors during defined treatment intervals, and using sequential PET scans to assess metabolic changes induced by the combination. We believe that understanding the correlations between downregulation of tissue biomarkers and quenching of the metabolic signal as assayed by the PET scan can help us develop a new paradigm to establish the range of biologically effective doses of novel agents. This is particularly important as assessment of targeted therapies is likely to differ substantially from the development of cytotoxic agents. Downregulation of key signaling pathways (assessed in serial tumor biopsies and correlated with PET imaging) will allow us to see if Akt is upregulated after the initial mTOR inhibitor and then quenched in human subjects after subsequent treatment with an IGFR TKI. It is not only important to assay these biological and pharmacological parameters for therapy of established advanced disease, it is also critical that we determine tolerable doses of IGFR/mTOR inhibitor combinations for long-term chemoprevention of individuals at high risk for development of lung cancer.

By developing this potentially potent combination of mTOR and IGFR inhibitors in parallel, we believe we can make important inroads into developing clinically meaningful data to potentially benefit populations at risk in the long term, while deriving relevant biological data about targeting important pathways that have, to date, been resistant to therapeutic intervention. This report describes the progress for the eighth grant year (March 15, 2008 to March 14, 2009), and third and final year of an unfunded extension from the Department of Defense (DoD).

PROGRESS REPORT

Project 1: Study Mechanisms of Molecular Alterations in Lung Cancer
(PI: Li Mao, M.D.)

Specific Aim 1 **To determine the mRNA complex responsible for C-CAM1 splicing and identify factor(s) regulating exon 7 splicing.**

This Aim was completed as reported in 2005.

Specific Aim 2 **To determine function of identified splicing factor(s) in regulation of CEACAM1 and its potential alterations in lung cancer.**

This Aim was completed as reported in 2005.

Specific Aim 3 **To determine function of DNA methyltransferases and their role in controlling methylation and expression of critical tumor suppressor genes and tumor antigen genes.**

This Aim was completed as reported in 2004.

Specific Aim 4 **To determine expression and abnormalities of DNMT3B isoforms in lung tumorigenesis and their association with de novo DNA methylation patterns, and clinical applications.**

This Aim was completed as reported in 2006.

Specific Aim 5 **To determine expression of hnRNP-A1 variants in lung cancer cells and their role in the regulation of pre-mRNA splicing.**

This Aim was completed as reported in 2007.

Specific Aim 6 **To determine the role of hepatoma-derived growth factor (HDGF) in lung cancer.**

This Aim was completed as reported in 2006.

Conclusions

We have concluded this project. The research has demonstrated the importance of ΔDNMT3B, a novel subfamily of DNMT3B discovered in the project, in lung tumorigenesis, the important role in regulation of promoter methylation, and identified HDGF as a key factor in lung cancer progression. These discoveries are progressing to the clinic through continued research now supported by an R01 and licensing agreements.

Project 2: Develop Novel Strategies for Lung Cancer Chemoprevention
(Project Leader: Fadlo Khuri, M.D.)

***Revised* Specific Aim 2.1 To determine whether treatment of lung cancer cells with mTOR inhibitors enhances dependence of these cells on survival signaling via IGFR**

mTOR inhibition-induced Akt activation appears to depend on IGF-1R in certain types of cancer cells. Thus, inhibition of IGF-1R signaling augments mTOR inhibitors' anticancer activity in these cell lines [10-12]. However, the synergy effect and the effective application sequence of mTOR and IGF-1R inhibitors in human lung cancer have not been documented. We will test how IGF-1R is involved in mediating Akt activation induced by mTOR inhibition in human lung cancer cells (Aim 1a) and whether co-inhibition of mTOR and IGF-1R signaling augments efficacy against lung cancer (Aim 1b). It has been documented that IGFR/EGFR heterodimerization counteracts the antitumor action of TKIs, whereas high levels of IGF-1R levels are associated with EGFR overexpression in human lung cancers [29, 30]. Moreover, IGF-1R signaling can activate the Raf/ERK MAPK pathway through EGFR [31, 32]. EGFR mutations impact lung cancer response to EGFR TKIs; however, the impact of the EGFR mutations on the co-targeting of mTOR and IGF-1R signaling remains unclear. Therefore, we will determine whether EGFR mutations impact cell sensitivivity to the combination of mTOR and IGF-1R inhibitions (Aim 1c).

Sub-Aim 1a. Determine whether IGF-1R is involved in mediating Akt activation by mTOR inhibition in human lung cancer cells.

Sub-Aim 1b. Determine whether co-inhibition of mTOR and IGF-1R signaling augments efficacy against lung cancer.

Sub-Aim 1c. Determine whether EGFR mutations impact cell sensitivity to co-targeting of mTOR and IGF-1R.

Summary of Research Findings

In this project, we proposed to use the IGF-1R tyrosine kinase inhibitor OSI-906 (OSI Pharmaceuticals); however, we had significant difficulty obtaining this compound due to intellectual property issues with the company. Alternatively, we obtained the IGF-IR antibody R1507 from Roche, which blocks IGF-1R signaling. Unfortunately, this antibody has minimal single agent activity against non-small cell lung cancer cells, and did not show enhanced growth inhibitory effects when combined with the mTOR inhibitor rapamycin or RAD001 in several tested human lung cancer cell lines.

We recently obtained BEZ235 from Novartis, which is a PI3K and mTOR dual inhibitor. In our proposal, we originally considered BEZ235 as our back-up or alternative plan. Through testing the effects of BEZ235 in human lung cancer cells, we found that BEZ235 very effectively inhibited the growth of a panel of human lung cancer cells. The IC_{50}s for a 3-day assay are between 2-15 nM (Fig. 1). Interestingly, the rapamycin-resistant cell line A549-RR did not exhibit any resistance to BEZ235; rather, A549-RR was even more sensitive to BEZ235 (Fig. 2). The IC_{50}s of BEZ235 in A549 parental cells (A549-P) and A549-RR were approximately 10 nM and 3 nM, respectively. These findings are somehow surprising because BEZ235 inhibits mTOR signaling as well, based on the information in the literature and provided by the company. Given that the rapamycin-resistant A549-RR cells exhibit very high levels of p-Akt due to mTOR inhibition-induced activation of PI3K signaling as we demonstrated previously (Wang et al., *Cancer Research* 2008), it is

plausible to suggest that mTOR inhibition with an mTOR inhibitor may induce dependence of lung cancer cells on the PI3K survival signaling, or addiction of lung cancer cell to the PI3K survival signaling, and thus enhance cell sensitivity to PI3K inhibition.

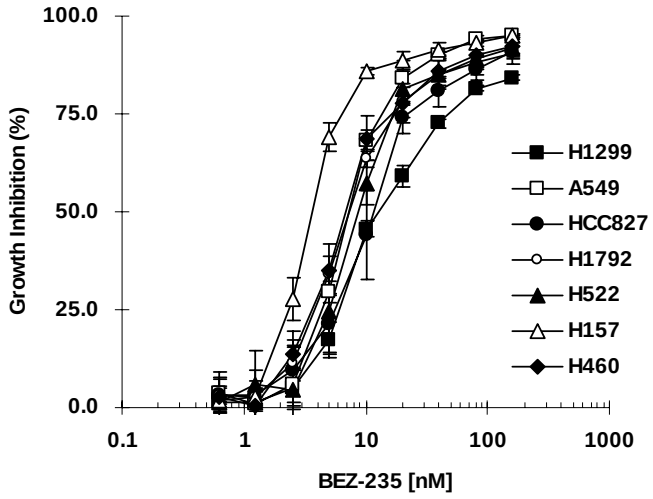

Figure 1: BEZ235 effectively inhibits the growth of human lung cancer cells. The indicated cell lines were treated with the given concentrations of BEZ235 for 3 days. The cells were then subjected to SRB assay for estimating cell number. Each data point represents the mean ± SD of four replicate determinations.

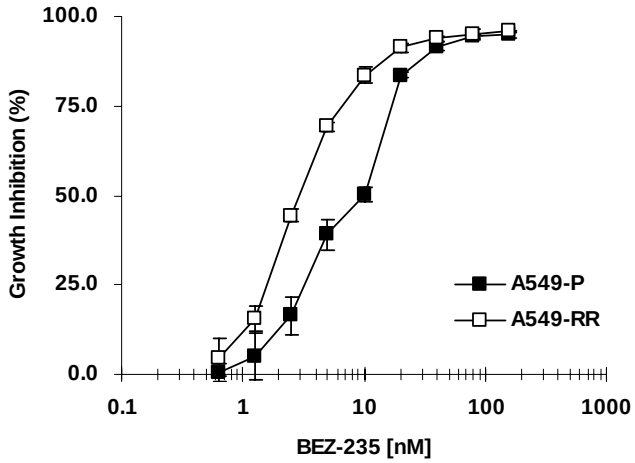

Figure 2: BEZ235 effectively inhibits the growth of rapamycin-resistant cells. The indicated cell lines were treated with the given concentrations of BEZ235 for 3 days. The cells were then subjected to SRB assay for estimating cell number. Each data point represents the mean ± SD of four replicate determinations.

Revisions to Proposed Aim and Future Plans

Based on our findings, we revised our aim to test the hypothesis that treatment of lung cancer cells with mTOR inhibitors enhances dependence of these cells on PI3K survival signaling. Thus, we will conduct the following experiments to fulfill our aim:

1. Test the anticancer effects of the sequential treatment with an mTOR inhibitor followed by a PI3K inhibitor (e.g., RAD001 followed by BEZ235) in cell-culture systems and in xenograft models.
2. Test the impact of PTEN mutation, PI3KCA mutation, or p-Akt levels on cell sensitivity to BEZ235.
3. Establish 1-2 additional rapamycin-resistant cell lines.

Through these studies, we hope to develop efficacious therapeutic regimens that target the PI3K/mTOR axis or overcome rapamycin resistance, which can be tested in clinical trials. We can also better test our novel approach of pharmacologically enhanced oncogene addiction. We plan to complete this additional proposed work over the next year; thus, a third and final no-cost extension has been requested for this project.

Key Research Accomplishments

- Demonstrated that the PI3K/mTOR dual inhibitor BEZ235 effectively inhibits the growth of human lung cancer cells.
- Reported enhanced sensitivity to BEZ235 in rapamycin-resistant cells.

Conclusions

Targeting the mTOR axis appears to be a promising strategy against lung cancer. However, development of rapamycin resistance is an important issue to be pursued in the clinic setting. Thus, the achievement of our research goal may allow us to develop novel strategies to enhance mTOR-targeted cancer therapy and prevent the development of rapamycin-resistance in cells.

Specific Aim 2.3. To investigate whether genetic approaches to inhibit PI3K activity decrease lung tumor size and number in k-ras mutant mice.

(PI: Ho-Young Lee, Ph.D.)

This Aim was discontinued as reported in the 2004 Annual Report due to the variability in the delivery system.

Specific Aim 2.4. To analyze differential gene expression between untreated NSCLC cells and celecoxib-treated NSCLC cells using affymetrix oligonucleotide microarrays and characterize genes that may be implicated in mediating apoptosis induction.

(PI: Reuben Lotan, Ph.D.)

This Aim was discontinued as reported in the 2008 Annual Report due to the challenges that have persisted with celecoxib use in the clinic.

Project 3: Implement Experimental Molecular Therapeutic Approaches for Lung Cancer
(Project Leader: Fadlo Khuri, M.D.)

Specific Aim 3.1 To develop a relatively faithful murine model of lung cancer by crossing the k-ras mutant mouse (T. Jacks) with p53 mutant missense mouse (G. Lozano) and study the evolution of non-small cell lung cancer in primary lung tumor model with metastatic potential and the effectiveness of targeted agents in the model.

(PI: Guillermina Lozano, Ph.D.)

This aim was completed as reported in 2008.

Specific Aim 3.2 **To evaluate novel signal transduction inhibitors alone, in combination with one another, or with cytotoxic agents in the treatment of the mouse lung cancer and, ultimately, in the treatment of human lung cancers.**

(PI: Fadlo Khuri, M.D.)

This aim was completed as reported in 2008.

Specific Aim 3.3 **To produce and test a liposomal gene-therapeutic strategy targeted to a novel tumor suppressor gene located on chromosome 3p, both in the mouse model and in human patients with advanced non-small cell lung cancer.**

(PI: Charlie Lu, M.D)

This aim was completed as reported in 2008.

Specific Aim 3.4 **To develop specific vascularly targeted strategies to the vascular endothelium of lung cancer cells to decrease the toxicity to normal cells and enhance the therapeutic index.**

(PI: Ho-Young Lee, Ph.D)

This aim was completed as reported in 2007.

Specific Aim 3.5 **To study in vivo and in vitro effects of farnesyl transferase inhibitors and tyrosine kinase inhibitors in mouse models and, ultimately, in humans with lung cancer.**

(PI: Guillermina Lozano, Ph.D.)

This aim was completed as reported in 2008.

Specific Aim 3.6 **To measure differences in gene expression between lung tumors that do or do not show metastasis, and in metastatic lesions themselves using the Affymetrix gene chip system.**

(PI: Guillermina Lozano, Ph.D.)

This aim was completed as reported in 2007.

Specific Aim 3.7 **To perform array CGH experiments to determine if other genomic changes have occurred.**

Specific Aim 3.8 **To perform LOH studies at specific loci (if warranted from the data obtained in Specific Aim 3.7).**

(Leader: Guillermina Lozano, Ph.D.)

These studies were dropped from the project due to lack of funds as reported in 2008.

Specific Aim 3.9 **To evaluate GFE-1 peptide effects on blocking lung metastases in a rat model.**

(PI: Yun W. Oh, M.D)

This Aim was concluded in 2005; Dr. Yun Oh discontinued participation in the BESCT program as noted in an official letter to Dr. Julie Wilberding at that time.

Conclusions

The tasks (Aims) of Project 3 have been completed.

Developmental Research Project: A Genetic/Combinatorial Algorithmic Strategy for Anticancer Therapy Development

(PI: Ralph Zinner, M.D)

Targeted therapeutic agents are highly promising in combination because they are both well-tolerated and interact with the targets that cause cancer. However, with new drugs added to the list, the number of possible combinations rises exponentially beyond the capacity of any foreseeable technology to fully screen. In addition, molecular insight often fails to predict clinical performance of single agents, a difficulty that will likely remain as these drugs are combined. We thus proposed a direct functional screen of combinations as a complement to the molecular insight-based approach, MACS (Medicinal Algorithmic Combinatorial Screen), to identify promising combinations that would be otherwise impossible to be found through a simple screen alone. The foundation of MACS is a genetic algorithm. The study adopts a preclinical screen that assesses anticancer efficacies of combinations with cell proliferation assays.

Specific Aim 1 To determine feasibility of screening process (robots, cell death assays, combining drugs).

Summary of Research Findings

This aim was completed as reported in 2008. Our manuscript detailing results for a screen with 19 different drugs using MACS has been published in *Molecular Cancer Therapeutics* (March 2009).

Specific Aim 2 To determine the range of outcomes and patterns of cellular response from an initial screening of drug combinations.

This aim was completed as reported in 2008.

Specific Aim 3 To develop a genetic algorithm to guide selection and identification of promising combinations of drugs.

This aim was completed as reported in 2007.

Conclusions

This study demonstrates the potential feasibility for screening drug combinations of arbitrary size using the Medicinal Algorithmic Combinatorial Screening (MACS) method, which can efficiently identify highly-fit combinations of anticancer agents without prior molecular or functional insight into the interactions of the combined drugs.

KEY RESEARCH ACCOMPLISHMENTS

Project 1: Study Mechanisms of Molecular Alterations in Lung Cancer

- All aims were completed and reported in 2007.

Project 2: Develop Novel Strategies for Lung Cancer Chemoprevention

- Demonstrated that the PI3K/mTOR dual inhibitor BEZ235 effectively inhibits the growth of human lung cancer cells.
- Reported enhanced sensitivity to BEZ235 in rapamycin-resistant cells.

Project 3: Implement Experimental Molecular Therapeutic Approaches for Lung Cancer

- All aims were completed and reported in 2008.

DRP: A Genetic/Combinatorial Algorithmic Strategy for Anticancer Therapy Development

- All aims were completed and reported in 2008.

REPORTABLE OUTCOMES

Manuscripts

Zinner RG, Barrett BL, Popova E, Damien P, Volgin AY, Gelovani JG, Lotan R, Pisano C, Lippman SM, Mills GB, Mao L, Miller JH. Algorithmic guided screening of drug combinations of arbitrary size for activity against cancer cells. *Molecular Cancer Therapeutics* 2009;8(3).March 2009.

CONCLUSIONS

In the 8th year grant period, all aims but one (Aim 2.1) have been successfully completed. Our current plan is to synergize with the complementary DoD Program BATTLE to both treat patients and to collect specimens to accomplish our original goals. Through these studies, we hope to develop efficacious therapeutic regimens that target the PI3K/mTOR axis or overcome rapamycin resistance, which can be tested in clinical trials. We can also better test our novel approach of pharmacologically enhanced oncogene addiction. We plan to complete this additional proposed work over the next year; thus, a no-cost extension has been requested for this project.

Project 1: This project has been completed with important discoveries in promoter methylation of ΔDNMT3B family members and the discovery of HDGF.

Project 2: The original goals of Aim 2.1 will best be served in a timely manner by synergizing with the research in the DoD Program BATTLE. Targeting the mTOR axis appears to be a promising strategy against lung cancer. However, development of rapamycin resistance is an important issue in the clinic. Thus, the achievement of our research goal may allow us to develop novel strategies to enhance mTOR-targeted cancer therapy or overcome or avoid the development of rapamycin-resistance.

Project 3: The tasks (Aims) of Project 3 have been completed.

DRP: The tasks of this study have been completed. The study demonstrated the potential feasibility for screening drug combinations of arbitrary size using the Medicinal Algorithmic Combinatorial Screening (MACS) method, which can efficiently identify highly-fit combinations of anticancer agents without prior molecular or functional insight into the interactions of the combined drugs. These findings have been recently published in *Molecular Cancer Therapeutics* (March 2009).

References:

1. Lippman, S.M., et al., Randomized phase III intergroup trial of isotretinoin to prevent second primary tumors in stage I non-small-cell lung cancer. *Journal of the National Cancer Institute*, 2001. 93(8): p. 605-18.
2. Khuri, F.R., et al., Retinoic acid receptor-beta as a prognostic indicator in stage I non-small-cell lung cancer. *Journal of Clinical Oncology*, 2000. 18(15): p. 2798-804.
3. Khuri, F.R., et al., Randomized phase III trial of low-dose isotretinoin for prevention of second primary tumors in stage I and II head and neck cancer patients. *Journal of the National Cancer Institute*, 2006. 98(7): p. 441-50.
4. Khuri, F.R., et al., Phase II trial of recombinant IFN-alpha2a with etoposide/cisplatin induction and interferon/megestrol acetate maintenance in extensive small cell lung cancer. *Journal of Interferon & Cytokine Research*, 1998. 18(4): p. 241-5.
5. Khuri, F.R., et al., A controlled trial of intratumoral ONYX-015, a selectively-replicating adenovirus, in combination with cisplatin and 5-fluorouracil in patients with recurrent head and neck cancer. *Nature Medicine*, 2000. 6(8): p. 879-85.
6. Khuri, F.R., et al., Multi-institutional phase I/II trial of oral bexarotene in combination with cisplatin and vinorelbine in previously untreated patients with advanced non-small-cell lung cancer. *Journal of Clinical Oncology*, 2001. 19(10): p. 2626-37.
7. Khuri, F.R., et al., Phase I study of farnesyl transferase inhibitor (FTI) SCH66336 with paclitaxel in solid tumors. *Clinical Cancer Research*, 2004. 10: p. 2968-2976.
8. Kim, E.S., et al., Phase II study of the farnesyltransferase inhibitor lonafarnib with paclitaxel in patients with taxane-refractory/resistant nonsmall cell lung carcinoma. *Cancer*, 2005. 104(3): p. 561-9.
9. Papadimitrakopoulou, V., et al., Phase I study of the farnesyltransferase inhibitor BMS-214662 given weekly in patients with solid tumors. *Clinical Cancer Research*, 2005. 11(11): p. 4151-9.
10. Morgillo, F., et al., Implication of the insulin-like growth factor-IR pathway in the resistance of non-small cell lung cancer cells to treatment with gefitinib. *Clinical Cancer Research*, 2007. 13(9): p. 2795-803.
11. Morgillo, F., et al., Heterodimerization of insulin-like growth factor receptor/epidermal growth factor receptor and induction of survivin expression counteract the antitumor action of erlotinib. *Cancer Research*, 2006. 66(20): p. 10100-11.
12. Fang, J., et al., Luteolin inhibits insulin-like growth factor 1 receptor signaling in prostate cancer cells. *Carcinogenesis*, 2007. 28(3): p. 713-23.
13. Roudabush, F.L., et al., Transactivation of the EGF receptor mediates IGF-1-stimulated shc phosphorylation and ERK1/2 activation in COS-7 cells. *Journal of Biological Chemistry*, 2000. 275(29): p. 22583-9.
14. Das AK, Sato M, Story MD, Peyton M, Graves R, Redpath S, Girard L, Gazdar AF, Shay JW, Minna JD, Nirodi CS. Non-small-cell lung cancers with kinase domain mutations in the epidermal growth factor receptor are sensitive to ionizing radiation. *Cancer Research*. 2006 Oct 1;66(19):9601-8.
15. Thomson, S., et al., Epithelial to mesenchymal transition is a determinant of sensitivity of non-small-cell lung carcinoma cell lines and xenografts to epidermal growth factor receptor inhibition. *Cancer Research*, 2005. 65(20): p. 9455-62.
16. Amann, J., et al., Aberrant epidermal growth factor receptor signaling and enhanced sensitivity to EGFR inhibitors in lung cancer. *Cancer Research*, 2005. 65(1): p. 226-35.

APPENDICES

APPENDIX A

Publications

Published Online First on March 10, 2009 as 10.1158/1535-7163.MCT-08-0937

Algorithmic guided screening of drug combinations of arbitrary size for activity against cancer cells

Ralph G. Zinner,[1] Brittany L. Barrett,[1] Elmira Popova,[4] Paul Damien,[5] Andrei Y. Volgin,[2] Juri G. Gelovani,[2] Reuben Lotan,[1] Hai T. Tran,[1] Claudio Pisano,[6] Gordon B. Mills,[3] Li Mao,[1] Waun K. Hong,[1] Scott M. Lippman,[1] and John H. Miller[7]

Departments of [1]Thoracic/Head and Neck Medical Oncology, [2]Experimental Imaging, and [3]Systems Biology, The University of Texas M. D. Anderson Cancer Center, Houston, Texas; [4]Department of Operations Research and Industrial Engineering and [5]Red McCombs School of Business, The University of Texas, Austin, Texas; [6]Sigma-Tau Pharmaceuticals, Inc., Rome, Italy; and [7]The Santa Fe Institute, Santa Fe, New Mexico

Abstract

The standard treatment for most advanced cancers is multidrug therapy. Unfortunately, combinations in the clinic often do not perform as predicted. Therefore, to complement identifying rational drug combinations based on biological assumptions, we hypothesized that a functional screen of drug combinations, without limits on combination sizes, will aid the identification of effective drug cocktails. Given the myriad possible cocktails and inspired by examples of search algorithms in diverse fields outside of medicine, we developed a novel, efficient search strategy called Medicinal Algorithmic Combinatorial Screen (MACS). Such algorithms work by enriching for the fitness of cocktails, as defined by specific attributes through successive generations. Because assessment of synergy was not feasible, we developed a novel alternative fitness function based on the level of inhibition and the number of drugs. Using a WST-1 assay on the A549 cell line, through MACS, we screened 72 combinations of arbitrary size formed from a 19-drug pool across four generations. Fenretinide, suberoylanilide hydroxamic acid, and bortezomib (FSB) was the fittest. FSB performed up to 4.18 SD above the mean of a random set of cocktails or ''too well'' to have been found by chance, supporting the utility of the MACS strategy. Validation studies showed FSB was inhibitory in all 7 other NSCLC cell lines tested. It was also synergistic in A549, the one cell line in which this was evaluated. These results suggest that when guided by MACS, screening larger drug combinations may be feasible as a first step in combination drug discovery in a relatively small number of experiments. [Mol Cancer Ther 2009;8(3):521–32]

Introduction

Combining chemotherapeutic agents is an established way to improve on single-drug efficacy, and small (two- to three-drug) combinations are now the standard of treatment for most metastatic cancers (1). Recent successes with larger multiple-agent regimens in the clinic (1, 2) encourage a continued search for improved combination chemotherapies; however, only a few of the virtually infinite possible combinations have been evaluated to date (3, 4) due to concerns about the potential toxicity of the combinations and the daunting logistics of testing all feasible combinations of available drugs (5).

The improved tolerability of new, potentially effective molecular targeted agents has encouraged combination of these agents with standard chemotherapy regimens and, more recently, with each other in early-phase clinical trials (1, 2, 6). In a recent review, it was observed that there is ''tremendous'' potential for improved therapy of cancer from combinations of molecular targeted agents designed to modulate different aspects of the same or different targets (7). Traditionally, strategies of combination drug development have been based on insights into non–cross-resistant molecular mechanisms of action, evidence of synergy, preclinical or clinical insights into nonoverlapping toxicities, and, more recently, insights into their effects on signaling pathways and host-tumor interactions (8, 9).

As a complement to these methods, we investigated the utility of a functional, laboratory-based screening of combinations. Laboratory-based screens have long been used to identify active single agents, and one company explored doublets using synergy (10). However, to our knowledge, there are no ongoing efforts to screen large spaces of potential combinations of more than two drugs. Extending a screen to larger cocktails may be useful given the time required to compile clinical evidence. However, *in vitro* assessments of any given cocktail become more challenging as drug combinations use larger numbers of agents. Moreover, even with highly efficient assessments of individual combinations, only a small fraction of the total possible cocktails can be evaluated given that they are

Received 9/29/08; revised 1/9/09; accepted 1/15/09; published OnlineFirst 3/10/09.

Grant support: Department of Defense BESCT Lung Cancer Program DAMD17-01-1-0689 (W.K. Hong).

The costs of publication of this article were defrayed in part by the payment of page charges. This article must therefore be hereby marked *advertisement* in accordance with 18 U.S.C. Section 1734 solely to indicate this fact.

Requests for reprints: Ralph Zinner, Department of Thoracic/Head and Neck Medical Oncology, Unit 432, The University of Texas M. D. Anderson Cancer Center, 1515 Holcombe Boulevard, Houston, TX 77030. Phone: 713-792-6363; Fax: 713-792-1220. E-mail: rzinner@mdanderson.org

doi:10.1158/1535-7163.MCT-08-0937

virtually countless. We made an effort to meet these challenges on two levels. First, we developed a rapid method, or fitness function alternative to synergy, to speed evaluation of individual cocktails. Second, we used a search algorithm intended to sequentially direct the screen toward increasingly more promising sets of drug combinations.

Fitness is a term used in search algorithms adapted from evolutionary theory. In biology, higher fitness describes an individual's greater capacity to reproduce. In search algorithms, it indicates a more optimal solution; what defines fitness is determined by the investigator and the problem that he or she is trying to solve. These algorithms guide a process through a finite list of operations intended to maximize fitness. Such algorithms have been extensively used outside medicine in applications such as data fitting, scheduling, trend spotting, and budgeting (11–13). They have been evaluated in medicine in breast cancer diagnosis (14) and in an antiviral *in vitro* model assessing a large space of dose permutations of a few cocktails (15). Here, a well-established strategy is applied to a novel setting: the discovery of drug cocktails. The algorithm works through a stepwise process of enriching successive pools of cocktails for increased fitness. It is this application we designate Medicinal Algorithmic Combinatorial Screen (MACS).

For MACS to be meaningful, fitness needs to predict a value of interest, and to be feasible, the fitness function needs to be efficient. We intended fitness to predict cocktail efficacy. Synergy is an established fitness function used for this purpose. Indeed, synergy was used by CombitoRx in evaluating doublets (10). However, synergy can become exponentially more labor-intensive with each drug added to a given cocktail. As an example, when six doses per drug are used, as done by CombitoRx,

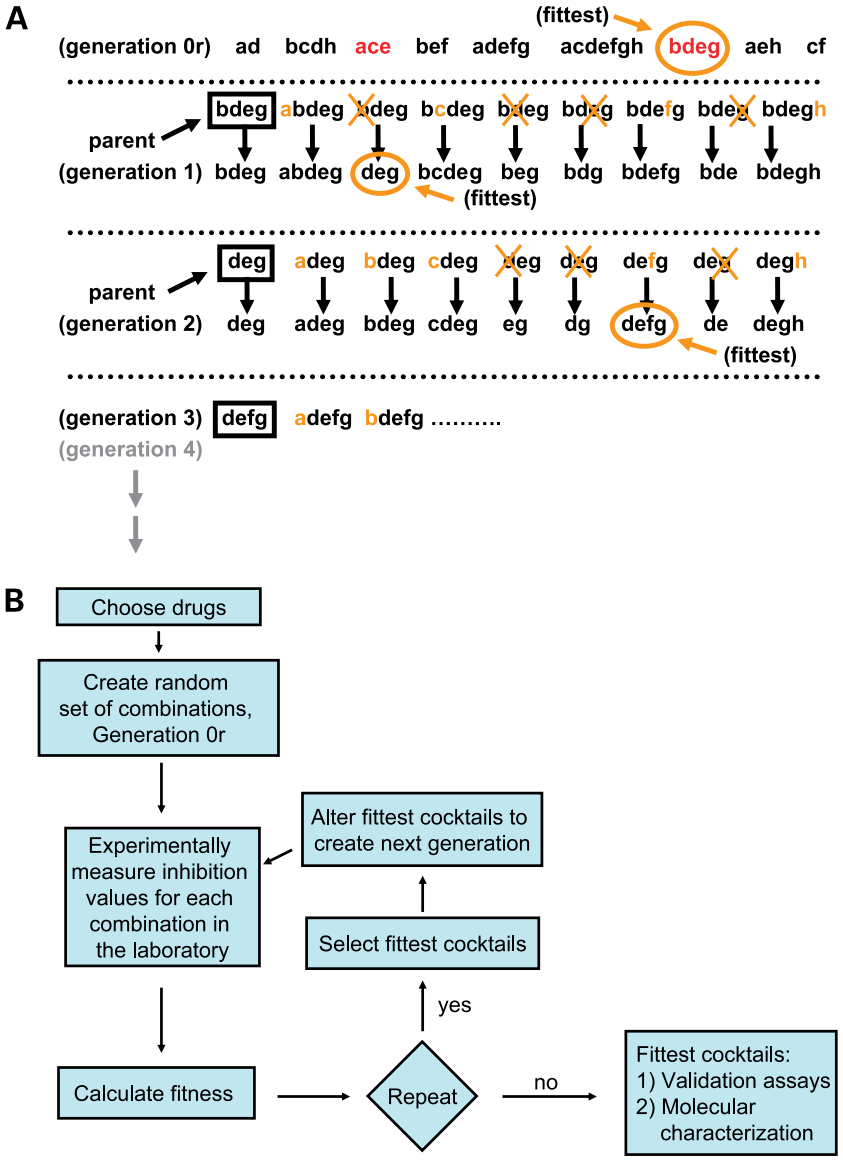

Figure 1. **A,** a model hill climb. Imagine an eight-drug pool with the drugs labeled ''a'' through ''h.'' In the initial generation (generation 0), 9 of 256 possible combinations are randomly formed. These combinations are, in turn, tested in cell culture. In this example, the combination identified as fittest is shown as ''bdeg.'' Note that we are not describing the fitness function here; different fitness functions can alter the fitness landscape and which among the nine would be determined to be fittest thereby altering the ultimate outcome. However, the rules of the hill climb will not be affected by the fitness function. Generation 1 is formed from the eight one-mutant combinations (also known as ''nearest neighbors'') of ''bdeg'' plus the parent. To form this generation, each of the eight drugs is added to or subtracted from the fittest combination in turn. Thus, because drug ''a'' is not present in the parent combination ''bdeg,'' it is added to form ''abdeg.'' Next, drug ''b'' is checked. Because it is already present in the parent, ''b'' is subtracted, resulting in the combination ''deg.'' This is repeated until all eight drugs are checked and generation 1 is formed, which is then tested. If ''deg'' were identified as the fittest combination, its eight nearest neighbors would then be determined, and so on. A local peak or maximum on the landscape is reached if none of the progeny are superior to the parent. **B,** a scheme outlining general steps characteristic of any MACS.

Table 1. The average activity of the single-agent controls across generations 0 to 3 hill climb

Agent (designation)	Drug class/mechanism of action	IC_{10} dose (μmol/L)	1× dose	2× dose	4× dose	Rank 1×	Rank 4×
Anisomycin	Protein synthesis inhibitor/activates JNK, p38 MAPK, and others	0.015	0.90	0.72	0.59	12	12
ATRA	**Retinoid: differentiation**	**15**	**0.87**	**0.74**	**0.63**	**8**	**16**
Bortezomib	**26S proteasome inhibitor**	**0.005**	**0.97**	**0.45**	**0.37**	**17**	**4**
CD437	Retinoid: proapoptotic	0.3	0.86	0.61	0.34	7	2
Cisplatin	Alkylating agent	5	0.85	0.72	0.51	5	9
Decitabine	DNA methylation inhibitor	2	0.88	0.84	0.78	10	17
Deguelin	Akt inhibitor	12	0.79	0.64	0.39	2	5
Fenretinide	**Retinoid: proapoptotic**	**5**	**0.86**	**0.66**	**0.19**	**6**	**1**
Gemcitabine	Antimetabolite	0.004	1.06	0.96	1.03	18	19
Imatinib	TKI of BCR-ABL, PDGF, c-kit	3	1.07	0.78	0.85	19	18
Indirubin	PKI*: GSK-3b, CDK5	1	0.92	0.69	0.51	15	10
LY294002	PI3K inhibitor	2	0.90	0.79	0.53	11	11
MX3350-1	Retinoid: proapoptotic	0.5	0.92	0.68	0.49	14	8
PD-168393	TKI: EGFR	5	0.85	0.63	0.47	4	7
Rapamycin	mTOR inhibitor	6	0.76	0.66	0.62	1	15
SAHA	**Histone deacetylase inhibitor**	**2**	**0.88**	**0.50**	**0.37**	**9**	**3**
SCH66336	FTI	5	0.90	0.78	0.59	13	13
SP600125	JNK1, -2, and -3 inhibitor	5	0.83	0.66	0.45	3	6
ST1926	Adamantyl retinoid: proapoptotic	0.05	0.95	0.90	0.60	16	14

NOTE: The three drugs in FSB and ATRA are in boldface. The 1× dose was the dose used in the MACSs. The levels of inhibition at the 1× and 4× doses are ranked and represent the average value across all generations (see Supplementary Fig. S2 for charts of each agent across the generations).
Abbreviations: ATRA, all-*trans* retinoic acid; SAHA, suberoylanilide hydroxamic acid; PKI, protein kinase inhibitor; TKI, tyrosine kinase inhibitor; PDGF, platelet-derived growth factor; EGFR, epithelial growth factor receptor; FTI, farnesyl transferase inhibitors; JNK, c-jun NH_2-terminal kinase; CDK5, cyclin-dependent kinase 5; MAPK, mitogen-activated protein kinase; PI3K, phosphatidylinositol 3-kinase; mTOR, mammalian target of rapamycin.

cocktails containing two, three, four, or five drugs generate 36, 216, 1,296, and 7,776 possible dose permutations, respectively. Although substantially smaller numbers of permutations could be managed by fixed dosing ratios or other ways of sampling, synergy may nonetheless remain daunting. Thus, we developed an alternative fitness function that required one assay per cocktail to improve the efficiency on the level of the individual cocktail. It was a composite of inhibition at a fixed dose of each drug and the number of drugs. Through the use of this novel fitness function, we lost information about a vast number of potentially informative dose combinations, but it enabled us to screen hundreds of unique cocktails per week. Other fitness functions could incorporate drug cost, anticipated toxicities, molecular insight, dose sequence, alternative dosing schemes, or any other characteristics of interest.

As with fitness functions that assess individual cocktails, there are countless possible search algorithms to guide screens of large sets of cocktails with different ones suited to varied combinatorial landscapes (Supplementary Fig. S1).[8] We present a simple example of such an algorithm called hill climbing (Fig. 1A; Supplementary Fig. S1).[8] This example does not represent actual data but rather illustrates a method. As can be seen in the figure, one can perform a MACS by sampling a relatively small subset of the possible cocktails (Supplementary Fig. S1).[8] Although the rules can vary among MACSs, they all entail a cycling between experimental evaluation of drug cocktails and a rule-based creation of the next generation (Fig. 1B). These rules involve selection and alteration. The selection function directs the choice of a subset of the cocktails tested, and in the case of the hill climb, the fittest one. However, it could choose more than one cocktail and even incorporate a stochastic element analogous to natural evolution in which fitness improves the odds of survival but offers no guarantees (as presented previously).[9,10] The alteration function can create all of the nearest neighbors of the selected cocktail(s), analogous to mutations as in the hill climb, or could combine pieces of different selected cocktails analogous to recombination.

Because any search of a large enough potential space will, for practical reasons, be confined to a small fraction of the total possible cocktails, it is likely that many of the fittest combinations will never be tested even when a search algorithm guides the process. The MACS needs only to find combinations that have fitness levels that are

[8] Supplementary material for this article is available at Molecular Cancer Therapeutics Online (http://mct.aacrjournals.org/).

[9] Zinner RG, Barrett BL, Volgin AY, Gelovani JG, Huang J, Tran HT, Mills GB, Hong WK, Fu Y, Mao L. Proc Am Soc Clin Oncol, 2005; abstract 2079.
[10] Miller JH, Zinner RG, Barrett BL. Directed discovery of novel drug cocktails. Sante Fe Institute Website 2005; 07-031, http://www.santafe.edu/research/publications/wpabstract/200507031.

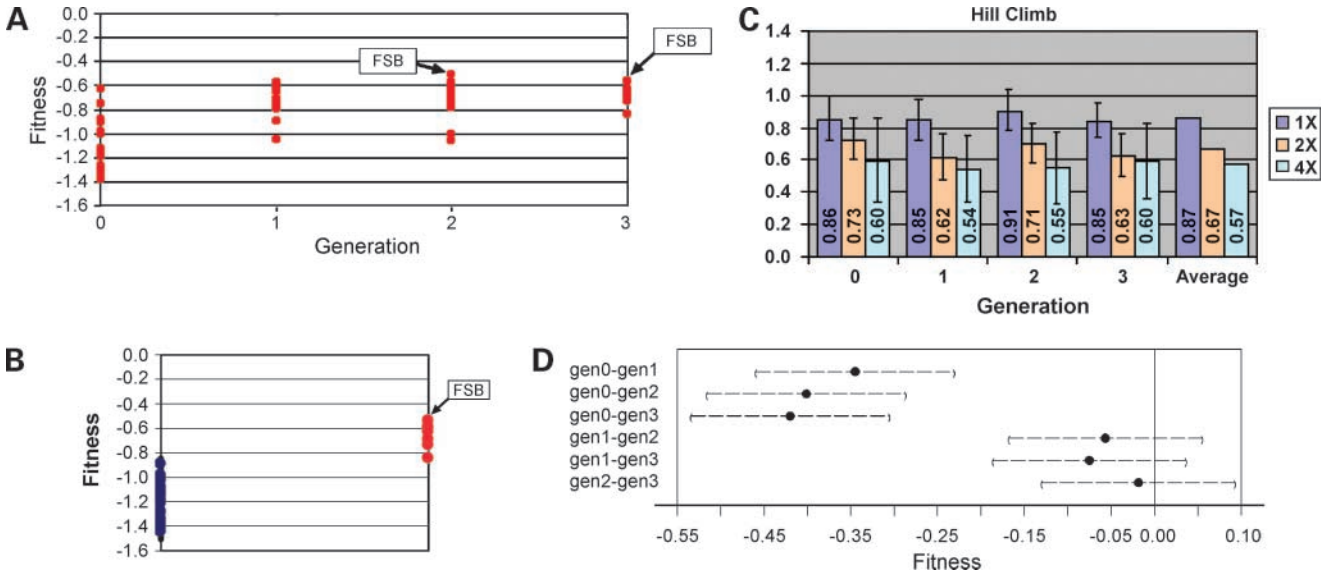

Figure 2. **A,** the performance of the hill climb. **B,** the set of cocktails composing the fittest cocktail and its nearest neighbors (or progeny) resulting from a local search compared with a set of randomly formed cocktails (described elsewhere).[9,10] **A** and **B,** the *x*-axis indicates the generation number, and in the *y*-axis, higher values indicate greater fitness level [not the inhibitory, K(s)]. **A,** the hill climb arrived at FSB by generation 2. Generation 3 includes FSB and its 19 nearest neighbors, which can be compared with the 18 randomly formed cocktails of generation 0. **B,** in blue is a set of 30 randomly formed cocktails; in red are FSB (the fittest cocktail) and its 19 nearest neighbors. This latter set is the same as the cocktails in generation 2 of the hill climb **A**, although the values in the hill climb represent a repeat assay of these cocktails. **C,** the average inhibitory values of the single-agent controls per generation are shown. The 1× values are the doses used in the MACSs. Note that the inhibitory values [or K(s)], not the fitness, are indicated along the *y* axis. The average values across all their respective generations are shown at the far right. For the individual values of each single-agent control across the generations, see Supplementary Fig. S3. **D,** multiple comparisons of the average fitness values and respective 95% confidence intervals of the generations from the hill climb.

''good enough'' more efficiently than a random screen to be useful.

In this proof-of-principle study, we developed a novel fitness function to evaluate cocktails and tested a number of different kinds of MACSs operating on combinations all derived from the same pool of 19 available anticancer drugs in an *in vitro* non–small-cell lung cancer (NSCLC) model. Based on data from earlier MACSs showing that a local search method such as a hill climb would be efficient (as compared with the more complex algorithms we evaluated earlier),[9,10] here we tested a hill climb-MACS. We then ran validation assays on the fittest identified cocktail in line with the general strategy in most drug development screens.

Materials and Methods

Unlike the model (Fig. 1A), the actual laboratory experiments composing the hill climb entailed 19 real agents creating a combinatorial space of 2^{19} or 524,288 possible cocktails. Eighteen cocktails were randomly formed for its generation 0 (as previously described[9,10]) and subsequent generations were created based on the assay results and the rules of the hill climb. The assay systems and conditions as well as fitness function were held constant throughout the hill climb-MACS.

Fitness Function

Our fitness function permitted one assay per cocktail to be done in triplicate. It was composed of a measured assay value representing inhibition and a nonmeasured value, a factor of the number of drugs in the cocktail. Starting at 0, 0.1 was subtracted for each 10% of cells remaining compared with the no-treatment controls. Thus, 70% inhibition yields 30% of the no treatment control value, or 0.3 to be subtracted. A ''penalty'' of 0.1 was assigned for each drug composing the cocktail based on the observation that each drug dosed at IC_{10} added to a cocktail increased inhibition by an average of 10% (data not shown). This penalty was designed to control for cocktail size to allow fitness to be determined by the cocktail composition.

Formally, fitness was $-K(s) - 0.1|s|$, where K(s) is the proportion of cells surviving relative to the no-treatment control and $|s|$ was the number of drugs in the cocktail. Fitness values thus can range from −0.1 (one drug kills all cells) to −2.9 (all 19 drugs with no inhibition). Even lower fitness values would be possible with growth stimulation relative to the untreated controls.

Selected Agents

Nineteen agents, 16 molecularly targeted and 3 chemotherapy, were used based on their availability, affordability, and ease of preparation and storage and the authors' experience in their use (Table 1; Supplementary Methods). Selected agents were required to inhibit A549 growth by at least 10% (IC_{10}) under the conditions used in the MACS (data not shown). A549 was chosen because it grows rapidly under uncomplicated laboratory conditions. Drugs requiring excessive concentrations of DMSO were excluded

given the independent ability of DMSO to inhibit A549 at doses of 1.7% by volume (data not shown). Drugs dissolved in ethanol were excluded because ethanol potentiated inhibition of A549 by DMSO.

Cell Lines

Eight human NSCLC cell lines were used to test the activity of the lead drug combination. A549, H226, Calu-3, H441, H1975, and HCC827 were purchased from American Type Culture Collection. HCC2279 was a gift from John Minna (Southwestern Medical School, Dallas, TX), and PC-14 was purchased from Riken BioResource Center. A549, H226, and Calu-3 cells were incubated in DMEM/F-12 (Invitrogen Corp.) containing 10% fetal bovine serum and 1% penicillin/streptomycin. H441, H1975, HCC827, HCC2279, and PC-14 cells were incubated in RPMI 1640 plus 10% fetal bovine serum.

Cells were isolated from BD Falcon 75-cm^2 tissue culture–treated flasks after a rinse with Cellgro PBS (Mediatech, Inc.) and the addition of Gibco trypsin-EDTA (0.05% trypsin, with EDTAx4Na) from Invitrogen. The cells were then plated at a volume of 50 μL/well in 96-well MicroWell Nunclon-Δ plates (Nalge Nunc International). Plated cells were then stored at 37°C in a humidified atmosphere containing 5% CO_2 until the drugs were added. The numbers of cells per well were as follows: A549, 1,500; H226, 3,000; PC-14, 2,500; HCC2279, 4,000; HCC827, 7,000; H441, 2,700; H1975, 6,000; and Calu-3, 15,000. All cell lines were incubated on Nunc 167008 96-well plates (Fisher Scientific International, Inc.).

Preparation of the Drug Combinations

Drugs for a given combination were mixed in a 96-well 2-mL sterile polypropylene block from Denville Scientific. All combinations were mixed at four times the volume needed for one well to allow for triplicate experiments and pipetting error. The final volume of DMSO (0.66%) in all wells, including the no treatment controls, was based on the maximum possible DMSO dose derived from the one cocktail containing all 19 drugs. Because each cocktail had its own individual DMSO volume, we added the unique additional DMSO individually to each cocktail, yielding 0.66% of a final volume of 250 μL. Medium was added to obtain a volume of 200 μL, which was in turn added to a well already containing the cells and media plated immediately before occupying 50 μL, yielding 250 μL.

Drug Doses

We used the single-agent IC_{10} dose (1× dose) regardless of the size of the combination because we anticipated that a higher IC value would result in maximal inhibition from many of the small cocktails, thereby reducing our ability to compare cocktails. All combinations were tested in triplicate in adjacent wells on the same plate, and each plate contained its own six untreated controls. All cocktails and controls were within the 60 non-edge wells to avoid an edge effect.[9,10] With each generation, we included 1×, 2×, and 4× single-agent controls in triplicate for all 19 drugs on a separate plate to check for consistency.

Preparation of Multiple Cell Lines

Cells were isolated from BD Falcon 75-cm^2 tissue culture–treated flasks after a rinse with Cellgro PBS (Mediatech) and the addition of Gibco trypsin-EDTA (Invitrogen). The cells were plated at a volume of 50 μL/well in 96-well MicroWell Nunclon-Δ plates (Nalge Nunc International). The numbers of cells per well were as follows: A549, 1,500; H226, 3,000; PC-14, 2,500; HCC2279, 4,000; HCC827, 7,000; H441, 2,700; H1975, 6,000; and Calu-3, 15,000. Cell lines were incubated on Nunc 167008 96-well plates (Fisher Scientific International). After the drug mixture was added, the plates were incubated for 44 h at 37°C in a humidified atmosphere containing 5% CO_2. This permitted reproducible measurements and a repeat assay during the workweek.

WST-1 Assay

Cell proliferation was measured using the WST-1 Cell Proliferation Reagent (Roche Diagnostics). After 44 h of incubation, 25 μL of WST-1 reagent were added constituting 9% of the well volume and the plates were incubated for another 4 h. The absorbance was measured on a scanning multiwell spectrophotometer at 440 nm with a 600-nm reference.

Preparation of FSB/ASB Subsets

All eight possible subcombinations of FSB—fenretinide, suberoylanilide hydroxamic acid, and bortezomib—(F, S, B, FS, FB, SB, FSB, no treatment control) and ASB in which fenretinide is replaced by all-*trans* retinoic acid (A, AS, AB, ASB) were tested in triplicate in eight NSCLC cell lines including A549. The doses were held stable in all cell lines at the IC_{10} for A549, and no edge wells were used. Each plate contained six untreated controls. An additional plate of A549 cells containing 1×, 2×, and 4× doses in triplicate of each drug and six no treatment controls was done with each experiment.

Synergy

We assessed the synergy of FSB in A549 and H2226 using all 64 possible dose combinations derivable from four dose levels: zero, 1× (high), 0.66× (medium), and 0.44× (low), done in triplicate. We used the same doses in each cell line to mirror the clinical case in which the drug titer in the serum affects the tumor as a whole unvaried from one clone to another. No edge wells were used and each plate contained six untreated controls. We also did single-agent controls on a separate plate at the 1× (high), 2×, and 4× doses for both cell lines. These values were also used in the synergy calculations. The combination index was calculated by the Chou-Talalay equation. In cases in which single agents stimulated growth, the value 0.000,001 was used to allow a calculation.

Statistical Analyses

No formal statistics were used to estimate the fitness. Statistical analyses of the MACS data and proliferation assays were carried out in Excel (Microsoft, Inc.) and SPlus (Insightful, Inc.) using ANOVA. The Kolmogorov-Smirnov test was run on the fitness values on sets of randomly formed cocktails. Analyses of synergy were done using CalcuSyn software (Biosoft Ltd.; refs. 16, 17).

A

Gen	Alteration	Cocktail	FSB	#Drugs	K(s)	Fitness	Fitness Rank	K(s) Rank
0	Random	Bor,Ly,Sa	SB	3	0.33	-0.63	1	5
0	Random	Bor,Cis,Ly,Sa,Sp	SB	5	0.25	-0.75	2	2
0	Random	At,Bor,Fen,Ima,Ly,Mx,Sa	FSB	7	0.18	-0.88	3	1
0	Random	At,Bor,Deg,Mx,Sa,Sp	SB	6	0.30	-0.90	4	4
0	Random	Ani,Deg,Ima,Pd,Sc		5	0.48	-0.98	5	10
0	Random	Cis,Ind,Rap		3	0.70	-1.00	6	13
0	Random	At,Dec,Ly,Sa,Sp	S	5	0.50	-1.00	7	11
0	Random	At,Bor,Cis,Dec,Fen,Ima,Sp	FB	7	0.43	-1.13	8	6
0	Random	At,Cis,Fen,Sp	F	4	0.73	-1.13	9	14
0	Random	Bor,Dec,Ima,Ly,Rap,Sp,St	B	7	0.44	-1.14	10	7
0	Random	Bor,Deg,Ind,Ly,Pd,Rap,Sp	B	7	0.44	-1.14	11	8
0	Random	Ly,Mx,Rap		3	0.88	-1.18	12	18
0	Random	At,Bor,Dec,Fen,Ly,Mx,Rap,Sp,St	FB	9	0.29	-1.19	13	3
0	Random	Ani,At,Dec,St		4	0.87	-1.27	14	17
0	Random	Cis,Fen,Ind,Ly,Mx	F	5	0.80	-1.30	15	15
0	Random	At,Dec,Ima,Ind,Mx,Sa	S	6	0.70	-1.30	16	12
0	Random	At,Dec,Fen,Gem,Ly,	F	5	0.83	-1.33	17	16
0	Random	An,At,Cd,Cis,Deg,Fen,In,Pd,St	F	9	0.48	-1.38	18	9
		Average Gen 0		5.56	0.54	-1.09		

B

Gen	Alteration	Cocktail	FSB	#Drugs	K(s)	Fitness	Fitness Rank	K(s) Rank
1	(-) LY294002	Bor, Sa	BS	2	0.38	-0.58	1	15
1	Parent	Bor,Ly,Sa	BS	3	0.28	-0.58	2	3
1	(+) Fenretinide	Bor,Ly,Sa,Fen	FBS	4	0.20	-0.60	3	1
1	(+) Cisplatin	Bor,Ly,Sa,Cis	BS	4	0.25	-0.65	4	2
1	(+) PD168393	Bor,Ly,Sa,Pd	BS	4	0.31	-0.71	5	4
1	(+) Rapamycin	Bor,Ly,Sa,Rap	BS	4	0.31	-0.71	6	5
1	(+) Deguelin	Bor,Ly,Sa,Deg	BS	4	0.34	-0.74	7	6
1	(+) SP600125	Bor,Ly,Sa,Sp	BS	4	0.34	-0.74	8	7
1	(+) MX3550-1	Bor,Ly,Sa,Mx	BS	4	0.35	-0.75	9	8
1	(+) Imatinib	Bor,Ly,Sa,Ima	BS	4	0.35	-0.75	10	9
1	(+) Gemcitabine	Bor,Ly,Sa,Gem	BS	4	0.35	-0.75	11	10
1	(+) Decitabine	Bor,Ly,Sa,Dec	BS	4	0.36	-0.76	12	11
1	(+) SCH66336	Bor,Ly,Sa,Sc	BS	4	0.36	-0.76	13	12
1	(+) Aniso	Bor,Ly,Sa,An	BS	4	0.37	-0.77	14	13
1	(+) CD437	Bor,Ly,Sa,Cd	BS	4	0.38	-0.78	15	14
1	(+) ST1926	Bor,Ly,Sa,St	BS	4	0.38	-0.78	16	16
1	(+) ATRA	Bor,Ly,Sa,At	BS	4	0.39	-0.79	17	17
1	(+) Indirubin	Bor,Ly,Sa,Ind	BS	4	0.39	-0.79	18	18
1	(-) SAHA	Bor,Ly	B	2	0.69	-0.89	19	19
1	(-) Bortezomib	Ly,Sa	S	2	0.85	-1.05	20	20
		Average Gen 1		3.78	0.39	-0.77		

Figure 3. This chart shows the performance of all the cocktails in the hill climb across the four generations. With the exception of generation 0, the second column indicates the changes to the parent cocktail to form its nearest neighbors with each change resulting in a given ''descendent.'' The column labeled ''FSB'' indicates which among the three drugs are embedded in the cocktail. K(s) cellular activity compared with the no-treatment control. A sample fitness value calculation is provided using Bor,Ly,Sa, $-(0.33 + 0.1(3)) = -0.66$. The cocktails are sequenced by fitness. The fittest cocktail is highlighted and becomes parent to the next generation. If one of the progeny is fittest, a new color is introduced. **A,** cocktails in generation 0 were formed randomly. **B, C** and **D,** the parent and its 19 progeny (nearest neighbors). Abbreviations are derived from the first two or three letters of the name of each drug.

Results

Fitness

An assessment of two sets of randomly formed cocktails showed that each additional drug increased inhibition by ~10%, supporting the 10% penalty for the fitness function (Supplementary Fig. S2).[8]

MACS

The hill climb-MACS arrived at the combination, FSB, in only three generations (generations 0–2). It was confirmed in the 4th generation (generation 3) as fittest in its immediate neighborhood after assaying a total of 72 unique combinations over 2 weeks (Figs. 2A and 3D).

C

Gen	Alteration	Cocktail	FSB	#Drugs	K(s)	Fitness	Fitness Rank	K(s) Rank
2	(+) Fenretinide	Bor,Sa,Fen	FBS	3	0.21	-0.51	1	1
2	(+) PD168393	Bor,Sa,Pd	BS	3	0.28	-0.58	2	2
2	Parent	Bor,Sa	BS	2	0.40	-0.60	3	14
2	(+) Rapamycin	Bor,Sa,Rap	BS	3	0.31	-0.61	4	3
2	(+) Cisplatin	Bor,Sa,Cis	BS	3	0.31	-0.61	5	4
2	(+) SP600125	Bor,Sa,Sp	BS	3	0.32	-0.62	6	5
2	(+) LY294002	Bor,Sa,Ly	BS	3	0.33	-0.63	7	6
2	(+) ATRA	Bor,Sa,At	BS	3	0.33	-0.63	8	7
2	(+) SCH66336	Bor,Sa,Sc	BS	3	0.33	-0.63	9	8
2	(+) Deguelin	Bor,Sa,Deg	BS	3	0.34	-0.64	10	9
2	(+) MX3550-1	Bor,Sa,Mx	BS	3	0.36	-0.66	11	10
2	(+) CD437	Bor,Sa,Cd	BS	3	0.37	-0.67	12	11
2	(+) Imatinib	Bor,Sa,Ima	BS	3	0.37	-0.67	13	12
2	(+) Indirubin	Bor,Sa,Ind	BS	3	0.40	-0.70	14	13
2	(+) Gemcitabine	Bor,Sa,Gem	BS	3	0.41	-0.71	15	15
2	(+) Aniso	Bor,Sa,An	BS	3	0.44	-0.74	16	16
2	(+) Decitabine	Bor,Sa,Dec	BS	3	0.44	-0.74	17	17
2	(+) ST1926	Bor,Sa,St	BS	3	0.49	-0.79	18	18
2	(-) Bortezomib	Sa	S	1	0.96	-1.06	19	20
2	(-) SAHA	Bor	B	2	0.91	-1.11	20	19
		Average Gen 2		2.78	0.43	-0.71		

D

Gen	Alteration	Cocktail	FSB	#Drugs	K(s)	Fitness	Fitness Rank	K(s) Rank
3	Parent	Bor,Sa,Fen	FBS	3	0.26	-0.56	1	7
3	(-) Fenretinid	Bor,Sa	BS	2	0.43	-0.63	2	18
3	(+) Indirubin	Bor,Sa,Fen,Ind	FBS	4	0.24	-0.64	3	1
3	(+) Deguelin	Bor,Sa,Fen,Deg	FBS	4	0.24	-0.64	4	2
3	(+) Cisplatin	Bor,Sa,Fen,Cis	FBS	4	0.25	-0.65	5	3
3	(+) PD168393	Bor,Sa,Fen,Pd	FBS	4	0.25	-0.65	6	4
3	(+) Aniso	Bor,Sa,Fen,An	FBS	4	0.26	-0.66	7	5
3	(+) Imatinib	Bor,Sa,Fen,Ima	FBS	4	0.26	-0.66	8	6
3	(+) SP600125	Bor,Sa,Fen,Sp	FBS	4	0.26	-0.66	9	8
3	(+) ST1926	Bor,Sa,Fen,St	FBS	4	0.26	-0.66	10	9
3	(+) Decitabine	Bor,Sa,Fen,Dec	FBS	4	0.27	-0.67	11	10
3	(+) LY294002	Bor,Sa,Fen,Ly	FBS	4	0.27	-0.67	12	11
3	(+) ATRA	Bor,Sa,Fen,At	FBS	4	0.27	-0.67	13	12
3	(+) MX3550-1	Bor,Sa,Fen,Mx	FBS	4	0.27	-0.67	14	13
3	(+) Rapamycin	Bor,Sa,Fen,Rap	FBS	4	0.28	-0.68	15	14
3	(+) CD437	Bor,Sa,Fen,Cd	FBS	4	0.28	-0.68	16	15
3	(+) Gemcitabine	Bor,Sa,Fen,Gem	FBS	4	0.29	-0.69	17	16
3	(-) SAHA	Bor, Fen	FB	2	0.51	-0.71	18	19
3	(+) SCH66336	Bor,Sa,Fen,Sc	FBS	4	0.33	-0.73	19	17
3	(-) Bortezomib	Sa,Fen	FS	2	0.64	-0.84	20	20
		Average Gen 3		3.78	0.30	-0.68		

Figure 3 *Continued*.

This is the same cocktail identified from MACSs described elsewhere.[9,10] We compared FSB and its nearest neighbors to two separate sets of randomly formed cocktails: 18 cocktails forming generation 0 of the hill climb and 30 cocktails derived from earlier experiments.[9,10] To compare to the 18 cocktails, we used the lower of two fitness values for FSB from generation 3 in the hill climb [K(s) = 0.26; fitness, −0.56]. FSB was 2.57 SD above the mean of its generation 0 (mean, −1.09; SD, 0.207) or in the upper 0.51% of the distribution. We had previously compared this same set (FSB and its nearest neighbors) by testing it the same day as the 30 randomly formed cocktails.[9,10] FSB [K(s) = 0.24; fitness, −0.54] performed 4.18 SD above the mean or in the upper 0.0014% of the distribution of these 30 cocktails assuming a normal distribution of fitness levels (Fig. 2B).[9,10] A Kolmogorov-Smirnov test on multiple sets of randomly formed cocktails derived from these earlier experiments

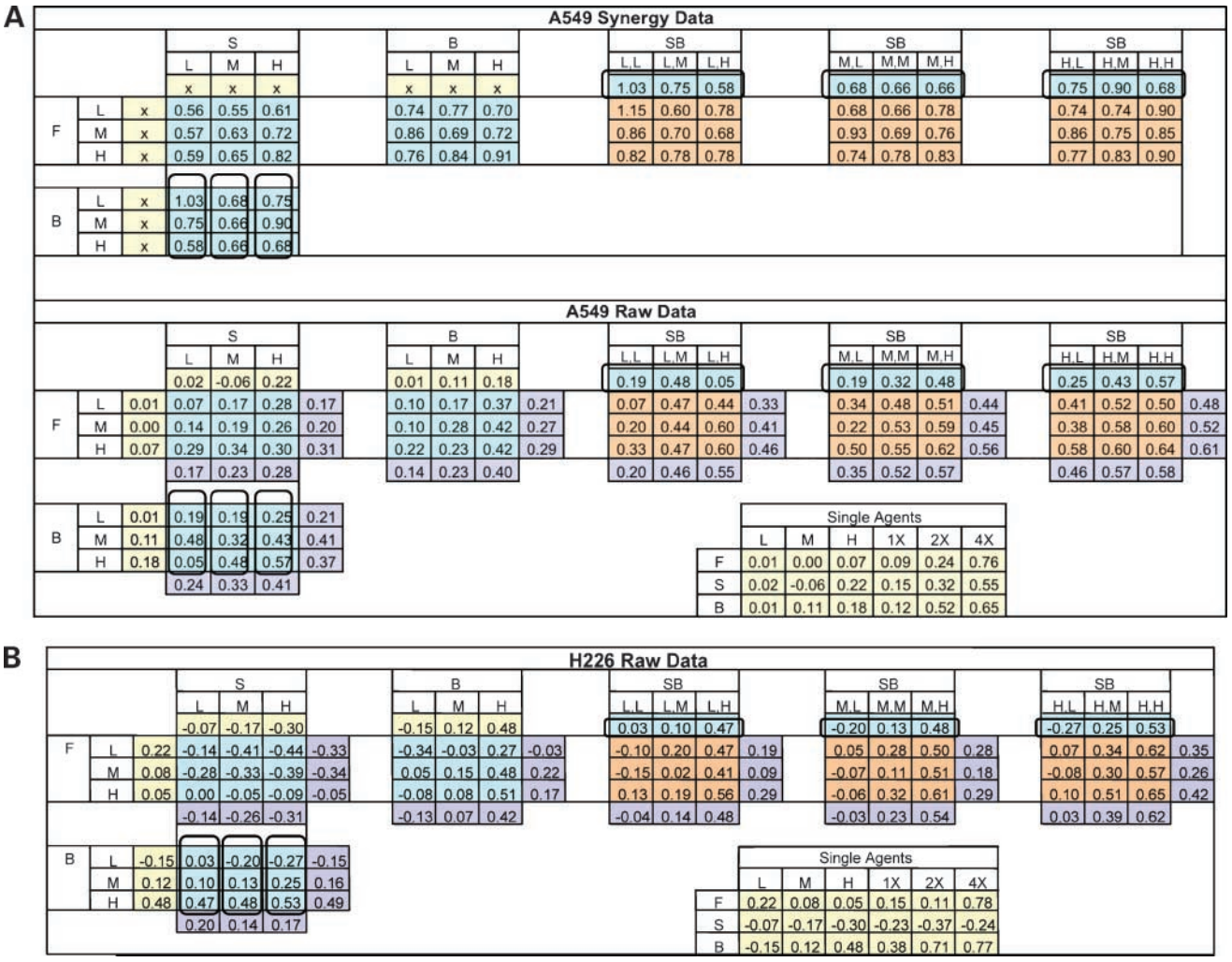

Figure 4. **A,** the synergy values and corresponding raw data for A549. **B,** the raw data for H226. The drugs and relative doses are indicated at the left and above. **A** and **B,** *yellow,* single agents; *blue,* doublets; *tan,* triplets; *purple,* averages. SB dose combinations are shown twice and are indicated using the rounded rectangles. Single-agent doses used in combination and the additional doses used in the controls are listed together below. *L,* low; *M,* medium; *H,* high; *H* is the same dose as 1×; *F,* fenretinide; *S,* suberoylanilide hydroxamic acid; and *B,* bortezomib. Synergy is indicated by a value <1. For raw data, values are equal to the fraction; inhibition, respectively, and negative values indicating stimulation.

(including the 30 mentioned above) produced a P value of 0.5, indicating a close approximation of normality.

In the hill climb, there was stability of the single-agent controls across the generations (Fig. 2C; Supplementary Fig. S3)[8] but a statistical improvement in the mean performance of the latter generations compared with the mean of the baseline generation (Figs. 2D and 3). Likewise, FSB and its nearest neighbors had a mean fitness value of −0.64 (SD, 0.07) compared with a mean fitness value of −1.18 (SD, 0.15) for the 30 randomly formed cocktails (Fig. 2B). Thus, the hypothesis that the means of the two distributions were the same was easily rejected (t = 17.1).

A closer look shows a steady enrichment for FSB. Among all 18 randomly formed cocktails from generation 0, the 6 most inhibitory cocktails contained a doublet derived from FSB (Fig. 3). In generation 1, if the parent, Bor,Ly,Sa, had inhibited slightly more, it would have been fittest and the hill climb would have stopped. By generation 2, all the nearest neighbors of BS were tested and FSB was fittest. In generation 3, FSB as parent was the fittest in its immediate neighborhood and the hill climb stopped. Note that subtraction of any of the drugs from FSB increased the K(s) sufficiently to render the doublets less fit. Moreover, addition of any drugs did not yield additional improvements in K(s) because FSB was maximally inhibitory under the laboratory conditions we used.

We compared FSB to 22 other triplets tested in an earlier MACSs.[9,10] The K(s) values were 0.43 to 0.99 (fitness, −0.73 to −1.29), compared with 0.18 − 0.26 (−0.48 to −0.56), among the six values for FSB in all MACSs.[9,10] FSB was also superior to an additional

20 triplets examined through the hill climb with K(s) 0.28 to 0.88 (−0.58 to −118; Fig. 3) although these triplets were highly enriched for FSB.

FSB was found to be synergistic in A549 (Fig. 4). In H226, synergy could not be calculated for most dose combinations given the single-agent stimulatory activity of suberoylanilide hydroxamic acid despite assigning a value of 0.000,001 to allow calculations (Fig. 4). This stimulatory behavior confirms earlier dose response results (Fig. 5A) and experiments discussed below (Fig. 5B). Although suberoylanilide hydroxamic acid increasingly stimulated H226, as its doses increased as a single agent and in combination with fenretinide, it had minimal effect when paired with bortezomib and magnified inhibition when combined with SB (Fig. 4).

Across all eight NSCLC cell lines, FSB was uniformly inhibitory, whereas the doublets were not and the single agents even less so (Fig. 5; Supplementary Table S1).[8] In all cases, FSB was more inhibitory than its constituent doublets. The substitution of all-*trans* retinoic acid, a congener of fenretinide, when averaging across all eight cell lines, yielded less inhibitory doublets and triplet despite the fact that all-*trans* retinoic acid, on average, was given at a more inhibitory single-agent dose than fenretinide (Supplementary Table S1).[8]

Discussion

To the best of our knowledge, this is the first study that shows the feasibility for screening drug combinations of

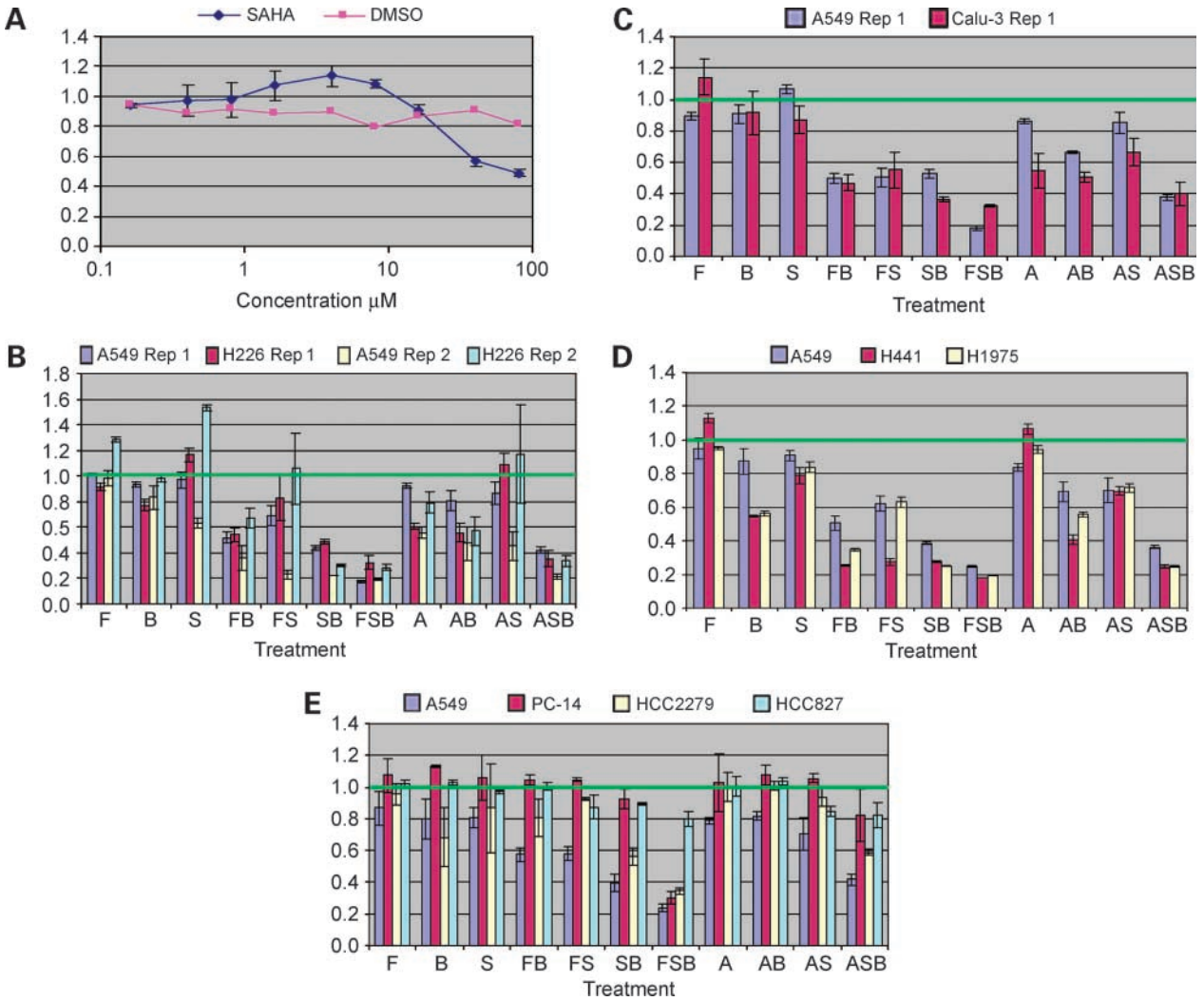

Figure 5. The results from the power sets (i.e., all possible subsets) of FSB (FSB, FS, FB, SB, F, S, B, and no-treatment control) and of ASB (ASB, AS, AB, SB, A, S, B, and no-treatment control) across multiple NSCLC cell lines are shown. The *y*-axis shows the ratio of the WST-1 value of the treated over the untreated control for a given cell line. Not shown are the A549 1×, 2×, and 4× single-agent controls that were done on the same day of all experiments. The set of seven other cell lines were set up on 4 separate days. On each of these days, A549 was used a control. **A,** dose-response curves for suberoylanilide hydroxamic acid (*SAHA*) in H226. The DMSO control titers match the increasing DMSO concentrations that increase as SAHA titers increase. **B,** A549 and H226. H226 with the A549 control was tested on 2 separate days and both sets of results are shown. **C,** A549 and Calu-3. **D,** A549, H441, and H1975. **E,** A549, PC-14, HCC2279, and HCC827. The numerical values are shown in Supplementary Table S1.

arbitrary size. It may also be the first using the strategy of a search algorithm–guided screen of cocktails (i.e., a MACS as described earlier[9,10]). The hill climb-MACS quickly and automatically identified a highly fit combination, FSB, the same cocktail identified in an earlier MACS.[9,10] It did so without the benefit of prior molecular insight into the interactions of the combined drugs. In addition, use of a novel fitness function substantially increased efficiencies at the level of the individual cocktail as compared with synergy thereby facilitating MACS in our lab.

Enrichment through the generations of sets of cocktails and the superior fitness of the FSB itself indicate that the hill climb-MACS was operating effectively (Fig. 2). This enrichment is also represented by the progressively increased presence of cocktails containing drugs derived from FSB, which were more inhibitory, a behavior that also indicates the upward directedness of the screen (Fig. 3). Similar behavior was also observed in the earlier MACSs.[9,10] Indeed, a MACS, whatever its rules, depends on the presence of a relationship between cocktail composition and fitness because the search has to ''learn'' from prior experience.

In the case of the hill climb-MACS, a triplet in the initial generation was highly enriched for FSB, by chance, placing it relatively high up a peak on the fitness landscape (Fig. 3A). This may in part explain the rapidity with which the hill climb identified FSB as well as its relatively low value of 2.57 SD above the mean fitness of its generation 0. Indeed, of 969 possible triplets, only 4 (0.41%), including FSB, contain at least two of the drugs. FSB at 4.18 SD above the mean needs to be interpreted with caution because the random set of 30 cocktails and its controls included edge wells whereas FSB and its nearest neighbors and controls did not (despite both sets being tested on the same day).[9,10] A number of post hoc analyses controlling for the edge effect yielded SD values ranging from 3.4 to >5 SD above the mean (data not shown). Even at 3.4 SD, FSB is still higher than would have been expected if cocktails were randomly tested (368 cocktails were evaluated through the earlier MACSs). The interpretation of the significance of the number of SD also depends on the assumption of a normal distribution of fitness values. Although an analysis of a larger set of 60 randomly formed cocktails showed a close statistical approximation to normality, we expect the tail of the distribution to ''fatten'' as cocktails fully inhibit by being quite large. Nonetheless, it does seem that FSB performed better than expected based on the above and other considerations.

In addition, FSB was substantially fitter than any of the other unrelated 22 triplets tested; thus, its fitness is not just a simple consequence of the fact that it is a triplet. Some caution is warranted because some of these triplets and their respective controls were tested using edge wells whereas FSB and its controls were not. However, the edge effect is substantially less than the observed differences in inhibition between FSB and the other triplets (data not shown).

The fact that FSB, which had been identified in an earlier MACS,[9,10] was identified a second time in the hill climb after screening only 72 cocktails was highly unlikely by chance given the space of a total of >500,000 potential cocktails and the many 10,000s of smaller potential cocktails. This also suggests that this particular fitness landscape is composed of a few higher peaks given the improbability of ascending the same peak twice by chance otherwise (Supplementary Fig. S1).[8] Interestingly, the hill climb nearly stopped at the triplet, Bor,LY,Sa, as it ascended the peak. Indeed, if by chance it had been a slightly more inhibitory value, the hill climb would have stopped. This indicates the potential benefit in performing a number of hill climb-MACS runs even with simpler landscapes.

With complex multipeaked landscapes, a hill climb-MACSs may arrive at different highly fit cocktails on different runs, thereby supplying a number of varied candidate cocktails (Supplementary Fig. S1).[8] However, such fitness landscapes, especially when composed of many lesser peaks, are often more successfully canvassed by more complex search algorithm–guided screens such as the hybrid algorithms we initially tested.[9,10] Indeed, future research can entail a determination of how factors such as assay type, constituent drugs, and varied fitness functions can influence the topography of fitness landscapes.

To speed the evaluation of individual cocktails, we used a fitness function alternative to synergy during the MACS. However, synergy remains important to consider given that it is a mainstay of current cocktail assessments and arguably more reliably predicts clinical efficacy because it integrates multiple dosing results per cocktail into a single synergy value. However, synergy experiments are increasingly labor-intensive as cocktails get larger with exponential increases in dose permutations. Moreover, such cocktails will likely have complex dose-response landscapes as hinted at by our results (Fig. 4). These likely cannot be neatly summarized by a synergy value. In addition, stimulatory values are not accommodated by standard synergy software, an issue that can arise even with single agents when using more than one cell line (Figs. 4 and 5A and B). One alternative to synergy to evaluate such dose-response combinatorial spaces is to use a search algorithm to guide a screen. This was recently reported by Wong et al. (15) on a space of 1,000,000 dose permutations derived from six drugs at 10 different doses per drug. Their strategy was similar to that used by us in this article and as previously described[9,10] but in their case instead directed at dose permutations. They used viral inhibition of a single-dose combination as a fitness value rather than synergy and applied a stochastic search algorithm to arrive at a highly fit dose combination. However, one could examine dose-response fitness data to identify regions of the space simple enough to perform standard synergy analyses. Such spaces may be yet more amenable to assessment using novel analytic synergy methods (18). Molecular insights may further direct analyses of this space.

Although the method reported by Wong et al. was highly efficient and reproducible, it required weeks to complete

a single run to arrive at the highly fit dose combination for a given cocktail. Their method applied to a large space of possible cocktails would thus be less speedy per cocktail, although more informative, than the fitness function we had used to evaluate individual cocktails. Future study can explore how to prioritize and optimize search efforts between the large space of different potential cocktails, as we have done, and the space of dose permutations per cocktail as done by Wong et al. (15). Yet other large combinatorial spaces formed from drug sequencing and altered dose durations, among others, may also merit exploration.

For MACS to be meaningful, the fitness result needs to be predictive. Future study could evaluate this including our fitness function, synergy, or any other function. Validation studies showing activity of FSB in multiple cell lines suggest some predictive potential of our simple fitness function. Moreover, it supports the hypothesis that combination therapy is more effective against a diversity of clones across patients and within heterogeneous tumors, a plausible observation given the experience in the clinic. There are also data from other labs supporting the positive interactions of some of the constituent doublets of FSB, although FSB seems to be a novel cocktail not previously studied (19–21). These reports indicate the power of existing and improving molecular insights in developing drug cocktails such as the doublets mentioned above. MACS is intended to complement current discovery methods for combination therapy based on molecular insights thereby speeding the existing process. It may also identify otherwise unanticipated candidate cocktails. Indeed, the potential to find cocktails unexpected by available insights is also indicated by results from a massive unguided screen of doublets by CombitoRx through which they found highly promising anticancer doublets formed from noncancer drugs (10).

The observation that there is a wide spectrum of NSCLC lines inhibited by FSB suggests a potential to inhibit host cells thereby drawing attention to the limitations of *in vitro* assays as predictors of toxicity. In the case of FSB, there are some clinical data indicating that FSB may be tolerable in the clinic (22–24). However, concerns for high risk of toxicity of drug cocktails argue the interest in development of *in vitro* toxicity assays, which in turn could be integrated into fitness functions and the MACSs. Indeed, the penalty we affixed to larger cocktails in our fitness function was a limited attempt to represent toxicity by favoring smaller cocktails. Whether FSB should be further developed or not, although there are substantial predictive limitations of existing *in vitro* assays, they are a foundation of drug development because they potentially offer some information of clinical value.

Separate from the question of feasibility and predictiveness of a fitness function are barriers to exploring the entire space of potential cocktails posed by limits in an assay. For example, we were unable to explore larger cocktails embedded with FSB, which, like FSB, maximally inhibited A549 but by definition were less fit. Alterations in assays or its conditions may expand the space of cocktails that can be meaningfully compared.

Although F, S, and B are not dosed at high single-agent inhibitory values relative to the other agents, they do have a disproportionately steep dose-response curve, with 4× dose inhibitory levels ranked 1st, 3rd, and 4th (all-*trans* retinoic acid was 16th; Table 1). MACS was not embedded with rules entailing prior knowledge of this attribute and yet efficiently found FSB. Nonetheless, such drug activity information or other functional data obtained through interrogating cocktail data sets generated during a MACS may usefully be embedded in a new algorithm or fitness function to improve MACS efficiencies.

Likewise, future MACSs could integrate biological insights by assigning a fitness ''reward'' for combinations that contain pairs of agents that are biologically tenable, or alternatively, one could choose pools of drugs that fit a molecular theme (or one could even use molecular rather than functional assays in the MACS). Contrariwise, MACSs founded in functional assays can be used to identify not only candidate therapeutics but also highly relevant candidate molecular probes. Insights derived from these probes could in turn be integrated into a new MACS, thereby forming a positive feedback loop of alternating MACSs and molecular evaluations. Limitations to molecular insights are exemplified by the fact that we would not likely have studied a fenretinide-containing regimen without a MACS given the recent diminished clinical interest in retinoids in lung cancer. They are also illustrated by the knowledge that all-*trans* retinoic acid is a congener of fenretinide and enabled only a limited capacity to predict efficacy (Supplementary Table S1).[8] Thus, successful MACSs would likely not limit exploration to molecularly tenable cocktails.

Further studies of combinatorial landscapes and search algorithms as well as the development of efficient fitness functions and improvements in laboratory gold standards and clinical models to evaluate promising candidates need to be developed. Even if MACS is shown elsewhere to be a useful strategy, the need to conduct a lengthy series of laboratory tests will remain, and if still promising, a series of evaluations through clinical trials of candidate cocktails. In addition, we note that there may be some challenges for widespread adoption of MACS, particularly the contractual or legal difficulties that may present when testing cocktails with agents owned by different entities. Principles derived from the development of MACS in this oncology setting may also be applied on a wider basis, such as modeling and assessing therapeutic candidates for infectious, rheumatologic, or other diseases, providing additional impetus to further development of this potentially advantageous screening strategy.

Disclosure of Potential Conflicts of Interest

No potential conflicts of interest were disclosed.

Acknowledgments

We thank Jean P. Issa, M.D., for kindly providing critical reagents; Dafna Lotan, M.S., for her superb assistance in drug preparation; Frank Fossella,

M.D., Mandri Obeyesekere, Ph.D., and Gabor Balazsi, Ph.D., for carefully reading the text and their highly insightful editorial suggestions; and Kathryn B. Carnes and Suzanne Davis, M.B.A., for excellent editorial assistance.

References

1. Sandler A, Gray R, Perry MC. Paclitaxel-carboplatin alone or with bevacizumab for non-small cell lung cancer. N Engl J Med 2006;355:2542 – 50.

2. Slamon DJ, Leyland-Jones B, Shak S, et al. Use of chemotherapy plus a monoclonal antibody against HER2 for metastatic breast cancer that overexpresses HER2. N Engl J Med 2001;344:783 – 92.

3. Frei E III, Eder JP. Principles of dose, schedule, and combination therapy. In: Holland JF, Bast RC, Morton DL, Frei E, Kufe DW, Weichselbaum RR, editors. Cancer medicine. Baltimore: Williams and Wilkins; 2006. p. 590 – 9.

4. Goldie JH, Codman AJ. A mathematical model for relating the drug sensitivity of tumors to the spontaneous mutation rate. Cancer Treat Rep 1979;63:1727 – 33.

5. Chu E, DeVita VT, Jr. Principles of cancer management: chemotherapy. In: DeVita VT, Jr., Hellman S, Rosenberg SA, editors. Cancer, principles and practice of oncology. Philadelphia: Lippencott Williams & Wilkins; 2001. p. 289 – 306.

6. Bendell JC, George D, Nixon A, Yu D, Hurwitz H. Results of a phase I study of bevacizumab (BV), everolimus (EV), and erlotinib (E) in patients with advanced solid tumors. Proc Am Soc Clin Oncol 2007;Abstract 3548.

7. Kwak EL, Clark JW, Chabner B. Targeted agents: the rules of combination. Clin Cancer Res 2007;13:5232 – 7.

8. Smith A. Screening for drug discovery: the leading question. Nature 2002;418:453 – 9.

9. Goodnow RA, Jr., Gillespie P. Hit and Lead identification: efficient practices for drug discovery. Prog Med Chem 2007;45:1 – 61.

10. Wadman M. The right combination. Nature 2006;439:390 – 401.

11. Holland JH. Adaptation in natural and artificial systems, 2nd ed. Ann Arbor: MIT Press; 1992.

12. Kirkpatrick S, Gelatt CD, Jr., Vecchi MP. Optimization by Simulated Annealing. Science 1983;220:671 – 80.

13. Abbas HA. An evolutionary artificial neural networks approach for breast cancer diagnosis. Artif Intell Med 2002;25:265 – 81.

14. Zheng B, Chang YH, Wang XH, Good WF. Feature selection for computerized mass detection in digitized mammograms by using a genetic algorithm. Acad Radiol 1999;6:327 – 32.

15. Wong PK, Yu F, Shahangian A, Cheng G, Sun R, Ho CM. Closed-loop control of cellular functions using combinatory drugs guided by a stochastic search algorithm. Proc Natl Acad Sci U S A 2008;105:5105 – 10.

16. Chou TC, Talalay P. Quantitative analysis of dose-effect relationships: the combined effects of multiple drugs or enzyme inhibitors. Adv Enz Regul 1984;22:27 – 55.

17. Chou TC, Motzer RJ, Tong Y, Bosl GJ. Computerized quantitation of synergism and antagonism of Taxol, topotecan and cisplatin against teratocarcinoma cell growth: a rational approach to clinical protocol design. J Natl Cancer Inst 1994;86:1517 – 24.

18. Fang HB, Ross DD, Sausville E, Tan M. Experimental design and interaction analysis of combination studies of drugs with log-linear dose responses. Stat Med 2008;27:3071 – 83.

19. Whang YM, Choi EJ, Seo JH. Hyperacetylation enhances the growth-inhibitory effect of all-trans retinoic acid by the restoration of retinoic acid receptor β expression in head and neck squamous carcinoma (HNSCC) cells. Cancer Chemother Phamacol 2005;56:543 – 55.

20. Denlinger CE, Rundall BK, Jones DR. Proteasome inhibition sensitizes non-small cell lung cancer to histone deacetylase inhibitor-induced apoptosis through the generation of reactive oxygen species. J Thorac Cardiovasc Surg 2004;128:740 – 8.

21. Touma SE, Goldberg JS, Moench P. Retinoic acid and the histone deacetylase inhibitor trichostatin a inhibit the proliferation of human renal cell carcinoma in a xenograft tumor model. Clin Cancer Res 2005;11:3558 – 66.

22. Schelman WR, Kolesar J, Schell K, et al. A phase I study of vorinostat in combination with bortezomib in refractory solid tumors. Journal of Clinical Oncology, 2007 ASCO Annual Meeting Proceedings Part I. Vol 25, No. 18S, 2007:3573.

23. Badros AZ, Philip S, Niesvizk R, et al. Grant Phase I trial of vorinostat plus bortezomib (bort) in relapsed/refractory multiple myeloma (mm) patients (pts). J Clin Oncol 2008;26:abstr 8548.

24. Costa A, Malone W, Perloff M, et al. Tolerability of the synthetic retinoid fenretinide (HPR). Eur J Cancer Clin Oncol 1989;25:805 – 8.